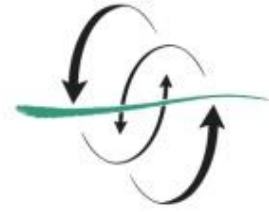


FACULTAD  
DE CIENCIAS  
DEL MAR



UNIVERSIDAD DE LAS PALMAS  
DE GRAN CANARIA

# **CO<sub>2</sub> FLUXES IN THE SOUTH AFRICAN COASTAL REGION**

**Veronica Arnone**

**Curso 2014/2015**

**Melchor González Dávila**

**J. Magdalena Santana Casiano**

Trabajo Fin de Título para la obtención  
del título: Grado en Ciencias del Mar

## CO<sub>2</sub> FLUXES IN THE SOUTH AFRICAN COASTAL REGION

*Datos personales del estudiante:*

**Veronica Arnone**

Grado en Ciencias del Mar

Curso 2014/2015

Universidad de Las Palmas de Gran Canaria, Facultad de Ciencias del Mar

e-mail: veronica.arnone101@alu.ulpgc.es

*Datos personales de los tutores:*

**Melchor González Dávila**

Universidad de Las Palmas de Gran  
Canaria,

Facultad de Ciencias del Mar

Departamento de Química

**J. Magdalena Santana Casiano**

Universidad de Las Palmas de Gran  
Canaria,

Facultad de Ciencias del Mar

Departamento de Química

En....., a.....de.....de 2015.

---

Estudiante: Veronica Arnone

---

Tutor: Melchor González Dávila

---

Co-tutora: J. Magdalena Santana Casiano

## CONTENTS

Abstract .....	1
1. Introduction .....	2
2. South African Coastal Region .....	4
3. Methods .....	7
3.1. System description .....	7
3.2. Fugacity of CO <sub>2</sub> determination .....	8
3.3. Computational method .....	9
4. Results .....	10
4.1. Hydrographic properties .....	10
4.2. Sea water fCO <sub>2</sub> .....	13
4.3. Fits of harmonic time functions .....	15
5. Discussion .....	16
5.1. Hydrographic properties .....	16
5.2. Fugacity of carbon dioxide .....	16
5.3. Trends of carbon dioxide .....	17
5.4. Limitation and future directions .....	18
6. Conclusion .....	18
Acknowledgments .....	19
References .....	20
Appendix .....	21

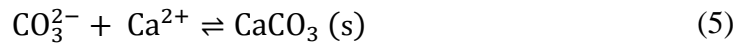
## Abstract

Surface water and atmospheric fugacity of carbon dioxide ( $f\text{CO}_2$ ) parameters were measured in the South African Coastal Region (18°25'E– 31°25'E) using volunteer observing ships (VOS) equipped with an automated underway  $x\text{CO}_2$  system. The ships operated along the QUIMA-VOS line in two different periods (2005-2008 and 2011-2012) and provided 16 records. From west to east the vessel track crossed three regions with different oceanographic conditions characterized by boundary currents and upwelling cells. Seasonal cycles of sea surface temperature (SST) and  $f\text{CO}_2$  integrated over each 0.5° presented a stable behavior with maximum values during Austral summer and minimum values during Austral winter related with climatological annual variability.  $f\text{CO}_2$  distribution showed saturated areas close to Cape Town, Port Alfred and, occasionally, Durban that acted as a  $\text{CO}_2$  source related with upwelling process. The area visited by the VOS line highlighted that this coastal region acted a sink of  $\text{CO}_2$  (mean  $\Delta f\text{CO}_2 = f\text{CO}_2, \text{sw} - f\text{CO}_2, \text{atm} = -33.05 \pm 34.07 \mu\text{atm}$ ). The interannual changes from 2005 to 2012 indicate that surface temperature decreased while fugacity increased over that period.

## 1. Introduction

Carbon dioxide (CO<sub>2</sub>) is one of the long-lived atmospheric greenhouse gases, whose global concentration is strongly determined by the marine environment. Seawater acts as a buffer and regulates the increase of atmospheric CO<sub>2</sub> that affects Earth's climate (Herr and Galland, 2009) and ocean chemistry. The carbon dioxide added to the atmosphere due to human activities, such as fossil fuel combustion and deforestation, is distributed within the land, air and sea. On time scales relevant to human societies the ocean carbon cycle is the largest active carbon reservoir.

Once CO<sub>2</sub> enters the ocean through the air-sea interface it dissolves in water and the reactions that take place can be summarized by a series of equilibria:



Nowadays, the global ocean remains generally mildly alkaline with surface water pH around 8.1-8.2 (Bates *et al.*, 2014; Doney *et al.*, 2009), where approximately 90% of the inorganic carbon is bicarbonate ion (HCO<sub>3</sub><sup>-</sup>), 9% is carbonate ion (CO<sub>3</sub><sup>2-</sup>), and only 1% is dissolved CO<sub>2</sub> (Doney *et al.*, 2009). However, the CO<sub>2</sub> uptake increases the aqueous CO<sub>2</sub>, bicarbonate, and hydrogen ion concentrations, resulting in gradual acidification of seawater. This also leads to a decrease of CO<sub>3</sub><sup>2-</sup> concentration and of the saturation state (Ω) of calcium carbonate (CaCO<sub>3</sub>) minerals like calcite and aragonite (Bates *et al.*, 2014). The chemical changes have a direct impact on marine organisms such as coral reefs, calcareous plankton and other organisms which form biogenic calcium carbonate. Currently, surface ocean pH is 0.1 units under pre-industrial conditions but predictions show that by the end of the century it will become 0.3-0.4 units lower (Orr *et al.*, 2005). These chemical changes and the inorganic carbon system can be characterized by measuring two of the four carbonate system parameters: pH, fugacity of carbon dioxide (fCO<sub>2</sub>), total alkalinity (TA) and total carbonate or total dissolved inorganic carbon (TCO<sub>2</sub>, DIC, C<sub>T</sub>).

In order to both predict the influence of anthropogenic “greenhouse gases” on future climate numerical models and check their performance, the results should be compared

with measurements. The quantity and quality of the existing data determine the progress. Since the beginning of the nineteenth century, seawater carbon dioxide measurements have been made but until the 1970s high quality data had not been obtained, especially before the start of the Geochemical Ocean Sections (GEOSECS) (1973-1979) and Transient Tracers in the Ocean (TTO) (1981-1983) programs (Doney *et al.*, 2009). During the 1990s three different programs were completed to understand ocean circulation, biogeochemistry and air-sea carbon exchange in order to provide the information that models needed. They were the World Ocean Circulation Experiment (WOCE), the Joint Global Ocean Flux Study (JGOFS), and the Ocean Atmosphere Carbon Exchange Study (OACES) (Key *et al.*, 2004). As described by Sarmiento and Gruber (2002), there are different models to predict futures potential concentrations of atmospheric CO<sub>2</sub> adjusted to diverse scenarios for anthropogenic emissions that lead to different results. The emission scenarios are full of uncertainties due to changes in population and human activities, technology development and the amount of ocean and land uptake.

Different studies show that from pre-industrial time the atmospheric carbon dioxide concentration has increased from about 277 parts per million (ppm) to 395 ppm now a days (Le Quéré *et al.*, 2014) but less than half of the emissions remain in the atmosphere (Slegenthaler and Sarmiento, 1993; Sarmiento and Gruber, 2002; Gruber *et al.*, 2009). The atmospheric growth is less than expected due to the ocean and terrestrial (plant and soil) uptake that represent the two primary sinks. Sabine *et al.* (2004) reports that from 1800 to 1994 the global atmospheric CO<sub>2</sub> sink accounted for  $118 \pm 19$  petagrams of carbon per year (Pg C/yr). The “Global carbon budget 2014” (Le Quéré *et al.*, 2015) reports different decadal means of the anthropogenic CO<sub>2</sub> budget highlighting sources and sinks. For 2004-2013, 91% of the total CO<sub>2</sub> emissions were caused by fossil fuel combustion and cement production and 9% by land use. The first caused a global carbon dioxide emission of  $9.8 \pm 0.4$  Pg C/yr versus  $0.9 \pm 0.5$  Pg C/yr from land use. During this decade, the growth rate of anthropogenic CO<sub>2</sub> was  $4.3 \pm 0.1$  Pg C/yr related to ocean and land sinks ( $2.6 \pm 0.5$  Pg C/yr and  $2.9 \pm 0.8$  Pg C/yr respectively). Compared to the 1960s means values are greater except land use emissions ( $1.5 \pm 0.5$  Pg C/yr). Fossil fuel combustion and cement production CO<sub>2</sub> emissions were  $3.1 \pm 0.2$  Pg C/yr causing together land use emissions an atmospheric carbon dioxide growth rate of  $1.7 \pm 0.1$  Pg C/yr. Ocean and land sinks were  $1.1 \pm 0.5$  Pg C/yr and  $1.8 \pm 0.7$  Pg C/yr.

Future conditions estimated with IS92a scenario for anthropogenic emissions of CO<sub>2</sub> led to different results depending upon the model used. By the end of 2100 atmospheric CO<sub>2</sub> concentration will be about 700, 713 or 980 ppm according to British Met Office’s Hadley Centre simulations. On the other hand, Lawrence Livermore National Laboratory ocean general- circulation model shows that atmospheric concentrations will exceed 780

ppm. Higher concentrations induce higher water temperature causing a decrease in solubility of gases, slower vertical exchanges and changes in the biological utilization of carbon (Sarmiento and Gruber, 2002). To sum up, global warming reduces sink strengths. Sabine *et al.* (2004) found that if  $p\text{CO}_2$  in surface waters continue to increase in proportion to atmospheric concentrations, this will lead to a 30% decrease in  $\text{CO}_3^{2-}$  concentrations and an increase of 60% in  $\text{H}^+$ .

Up to the present, air-sea  $\text{CO}_2$  exchange and the uptake by major oceans were largely studied but processes in coastal oceans are still poorly understood. Coastal waters and shelf seas link land, rivers, open ocean, atmosphere, biota and sediments, playing an important role in oceanic biogeochemical cycling. According to Chen *et al.* (2013), there is no consensus among the scientific community on whether continental margins act as a source or sink of  $\text{CO}_2$  but they appear to be spatially and temporally heterogeneous environments. Some studies reveal that marginal seas at high and temperate latitudes act as a sink of atmospheric carbon dioxide, in contrast to tropical and subtropical marginal seas that act as a source of  $\text{CO}_2$  (Borges *et al.*, 2005; Cai and Dai, 2004; González-Dávila *et al.*, 2009). Extrapolation based on limited shelf observations inferred a net coastal ocean uptake of about 0.4 Pg C/yr (Chen *et al.*, 2013; Cai and Dai, 2004; Borges *et al.*, 2005). The main factors that determine the  $\text{CO}_2$  concentration in coastal water are water temperature, river plumes, upwelling, wind and biological production.

The aim of this work was to study the spatial and seasonal variability of  $f\text{CO}_2$  in surface waters of the South African coastal sea in order to provide seasonal and interannual trends in carbon dioxide partial pressure and its role as sink or source of carbon dioxide exchange over the continental shelf. The information discussed derived from QUIMA-VOS line in situ measurements ([www.carboocean.org](http://www.carboocean.org) and [www.carbochange.b.uib.no](http://www.carbochange.b.uib.no)).

## 2. South African Coastal Region

African continental shelves are poorly examined, with only eight locations being studied, three of them located in South Africa, one in the Angola-Benguela region (González-Dávila *et al.*, 2009; Santana-Casiano *et al.*, 2009) and two in the southern coast at 35°42'S–20°6'E and 34°6'S–26°11'E (Chen *et al.*, 2013). Annual air-sea fluxes in the last two locations show that the continental shelf acts as a sink of atmospheric carbon dioxide ( $-2.41 \text{ mol C m}^{-2} \text{ yr}^{-1}$  and  $-4.03 \text{ mol C m}^{-2} \text{ yr}^{-1}$  respectively). Based on different measurements, the South African coastal region acted as a sink of atmospheric carbon dioxide but the estimation differs significantly with values from  $-4.03 \text{ mol C m}^{-2} \text{ yr}^{-1}$  to  $-2.41 \text{ mol C m}^{-2} \text{ yr}^{-1}$  according to Chen *et al.* (2013). It should be indicated that those studies only consider one (summer) and two (summer and autumn) seasons, respectively,

and data should be considered as estimative. As described by González-Dávila *et al.* (2009) the area south of 32°S acted as a sink of CO<sub>2</sub> with fluxes that changed between  $-1.17 \text{ mol C m}^{-2} \text{ yr}^{-1}$  and  $-3.24 \text{ mol C m}^{-2} \text{ yr}^{-1}$  (2006 and 2007 estimations). Santana-Casiano *et al.* (2009) estimations showed that 30°S also uptake CO<sub>2</sub> but with fluxes rates of  $-2 \text{ mol C m}^{-2} \text{ yr}^{-1}$  in August and  $-4 \text{ mol C m}^{-2} \text{ yr}^{-1}$  in November (2006). For both the Western Indian Boundary Current (from 27°S to 40°S) and the Eastern South Atlantic Boundary Current (from 35°S to 15°S) the estimated air-sea fluxes were  $1.0 \text{ mol C m}^{-2} \text{ yr}^{-1}$ , as reported by Chen and Borges (2009).

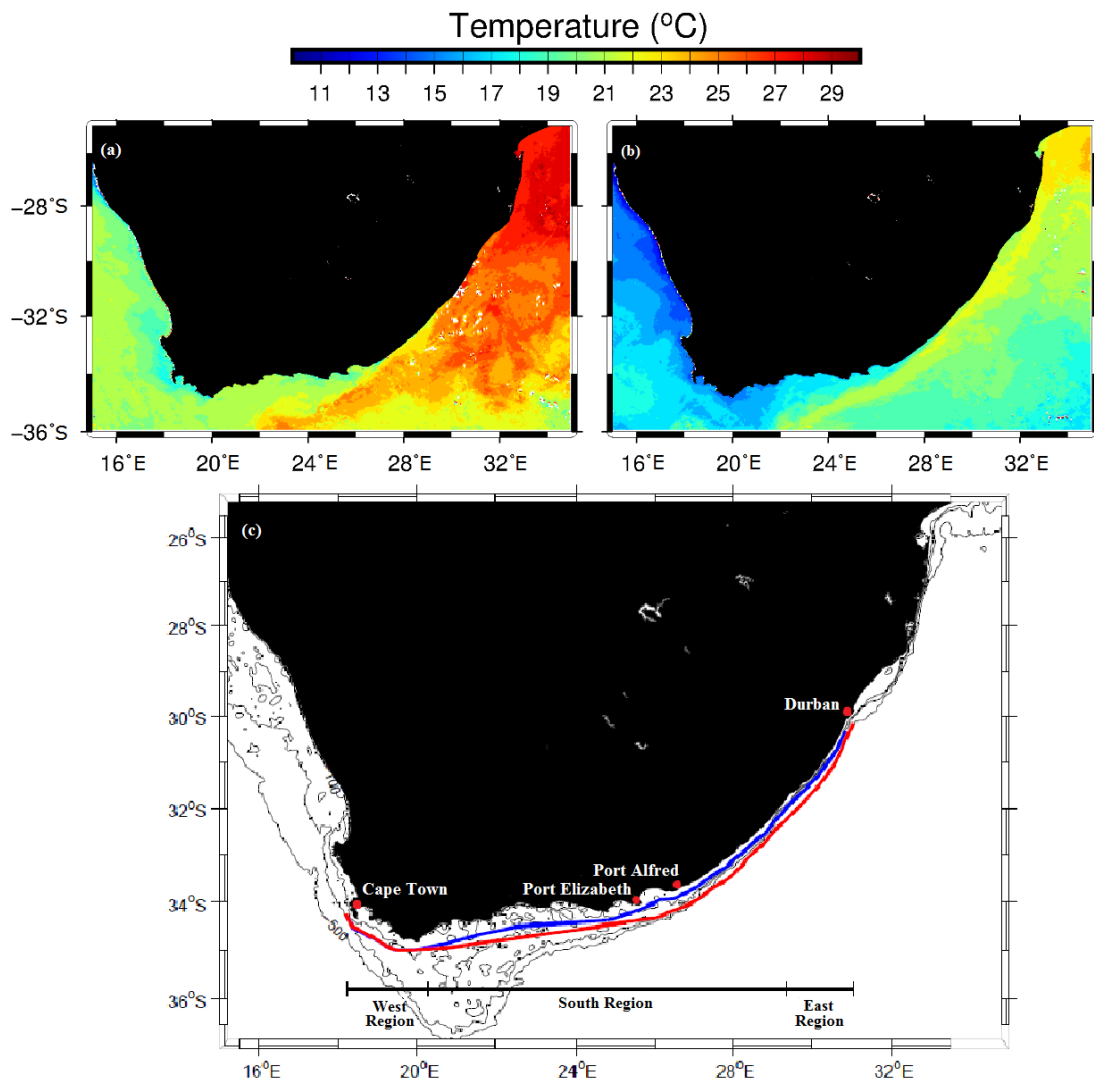


**Figure 1.** a) A MODIS satellite sea surface temperature image in January 2009 (8 day composite) showing a strong Agulhas Current flow southward on the east South Africa coast and a weak Benguela upwelling along the west, characteristic of the austral summer. b) A MODIS satellite sea surface temperature image in July 2009 (8 day composite) indicating cooler austral winter temperature with a weak Agulhas Current flow and a strong upwelling on the west. c) South Africa map with vessel track in blue (Cape Town–Durban) and red (Durban–Cape Town). The bottom black line indicates the longitudinal range of each Region considerate in this study.

The South African coastal region is characterized by 250 functional estuaries over an extension of 3,650 km (James *et al.*, 2013). The region is influenced by two boundary currents, the Benguela (eastern boundary current) on the west side and the Agulhas (western boundary current) on the east side, creating three different sections. In this study, the three regions are defined as West Region (18°25'E–20°25'E), South Region (20°26'E–29°25'E) and East Region (29°26'E–31°25'E), whose total extension covers part of the South African coastline, the one visited by the VOS line (Fig. 1c). The West Region is dominated by the Benguela upwelling produced by strong winds parallel to the shore that bring to surface South Atlantic Central Water (from 100 to 300 m), which is cool and nutrient rich (James *et al.*, 2013). In the northern Benguela region (north of ~28°S) water flows poleward with strong seasonality and is most intense during spring and summer. Across 30°S (southern Benguela region) the transport is equatorward during all seasons (Veitch *et al.*, 2010). Northern upwelling cells have lower seasonal variability than southern cells (summer upwelling peak). The South Region is an intermediate sector with great variability due to the influence of the surrounding areas. Lutjeharms *et al.* (2000) described the non seasonal upwelling of South West Indian Central Water (from 500 m) near Port Alfred (33°36'S–26°53'E) associated with the passing of a coastal jet from a narrow to a wider shelf and the wind stress. This water is characterized by salinity around 35.2 and temperature less than 13°C. Due to water stratification and the strength of the upwelling, water outcropped is partially mixed with surface water and their temperature lies between 14–17°C. During summer and spring surface water shows minimum temperatures related to wind-driven upwelling. Finally, the East Region is dominated by the Agulhas Current that flows strongly poleward bringing warm, nutrient-poor tropical water from the east of the western Indian Ocean. Water masses characteristic for this current are South Indian Tropical Surface Water (temperature over 22 °C) and South West Indian Subtropical Surface Water (temperature about 17.5 °C).

The Agulhas Current width and core position does not display an annual cycle and the path variations are related to the passage of offshore meanders at the inshore edge. The transport shows an annual variation, with a maximum in austral summer (February) and a minimum in austral winter (August). Their absolute geostrophic current speed varies from a mean of 1.4 m/s to a maximum of 2.8 m/s (Krug and Tournadre, 2013). As shown in Fig. 1a and 1b, the Agulhas Current system presents a clear seasonality influenced by monsoonal winds through the Mozambique Channel (Biastoch *et al.*, 1999). This variability also affects the climate of the region. The East coast has subtropical humid conditions due to the moisture and heat transfer between ocean and atmosphere that led to a peak of rainfall and river runoff in summer. The south coast shows a bimodal peak in rainfall during summer and winter (James *et al.*, 2013). The runoff controls the estuaries morphology and biogeochemical material cycles with direct implications for

primary production inside the estuary and in coastal waters. Rivers are the main source of nutrients and carbon to the estuaries and their values are governed by the residence time, water temperature, biogeochemistry and wind speed. Upper estuaries (salinity < 2) are usually found to be highly supersaturated in terms of pCO<sub>2</sub>, acting as source of carbon dioxide, while lower estuaries (salinity > 25) are less concentrated and act as sinks of atmospheric CO<sub>2</sub> (Chen *et al.*, 2013). Also, rivers plumes are found to act as sinks due to high photosynthetic rates. As reported by Chen *et al.* (2013), in the Agulhas Current region estuaries release  $4.95 \times 10^{-3}$  Pg C/yr while shelf surface uptake is  $12.28 \times 10^{-3}$  Pg C/yr.

The Agulhas system plays an important role in ocean circulation and climate. The leakage of warm and saline water from Indian to Atlantic Ocean through the Agulhas Current impacts the strength of the Atlantic Meridional Overturning Circulation (AMOC) (Beal *et al.*, 2011). This leakage is increasing under anthropogenic climate changes, and consequently is necessary to characterize the processes that take place in the Agulhas system and the potential climate change feedback.

### 3. Methods

#### 3.1. System description

Temperature, salinity and *f*CO<sub>2</sub> data were measured with an automated underway xCO<sub>2</sub> system developed by Craig Neill, installed onboard volunteer observing ships (VOS). The system mainly consists of three modules: (1) the “wet” box contains all components of the flowing seawater system including the equilibrator, the condenser and the water flow meter; (2) the “dry” box encloses the electronics components (the LICOR™ analyzer, computer and power supply); and (3) the “deck” box that includes a global positioning system (GPS). The computer checks the correct system performance, stores data, and puts the system into a sleep mode in user-selected areas by monitoring of GPS signal to avoid taking in contaminated port waters.

The seawater flows (over 60 l min<sup>-1</sup>) from the ship's uncontaminated seawater supply towards the plexiglass equilibrator (3 l min<sup>-1</sup>), where the water CO<sub>2</sub> content is equilibrated with the gas present in the chamber. After drying the equilibrator gas sample or the atmospheric air by passing the air through a Peltier system and NAFION® tubes, they are pumped to a non-dispersive, infrared analyser supplied by LICOR™ (Licor-6262 CO<sub>2</sub>/H<sub>2</sub>O analyzer) that evaluates seawater and atmospheric molar fraction of CO<sub>2</sub> (xCO<sub>2</sub>). Subsequently, the gas is returned to the equilibrator forming a closed loop (Pierrot *et al.*, 2009). The measurements are corrected for water vapor due to the drying

process before the determination, following DOE (1994). Every 3h the analyzer is calibrated with four different standard gases provided by the National Ocean and Atmospheric Administration (NOAA) and traceable to the World Meteorological Organization (WMO). The mixing ratios of standards are 0.0, 250 ppm, 380 ppm and 490 ppm of CO<sub>2</sub> in air (Santana-Casiano *et al.*, 2009).

Different types of sensors are used to analyse the sample properties and to control the correct equipment operation. In order to monitor the seawater intake and equilibrator temperature a SBE38 thermometer and a SBE21 thermosalinograph, respectively, are included in the system. A fraction of water intake is carried out by different channels to an oxygen sensor, to the thermosalinograph and to a fluorometer (Turner A10) (Santana-Casiano *et al.*, 2009). Measurement of temperature and pressure in the different system enclosures are important in order to determine fugacity of carbon dioxide ( $f\text{CO}_2$ ) values. All measurements are recorded in the system and downloaded at port.

Four different container cargo ships were used in the present study, the MSC-MARTINA, the MSC-GINA and the MSC-BENEDETTA from the Mediterranean Shipping Company (from 2005 to 2008) and LARS MAERSK from the Maersk Line company (between 2010 and 2013). All of them were operating on a route from Northern Europe via Las Palmas (where the data was collected) to South Africa, docking at Cape Town, Port Elizabeth and Durban. The equipment location in each vessel is different and that affects the temperature differences between the seawater intake and the TSG,  $0.23 \pm 0.05^\circ\text{C}$  on the MSC-MARTINA,  $0.06 \pm 0.01^\circ\text{C}$  on the MSC-GINA and MSC-BENEDETTA, and  $0.1 \pm 0.05^\circ\text{C}$  on the LARS MAERSK.

### 3.2. Fugacity of CO<sub>2</sub> determination

The  $(p\text{CO}_2)_{\text{T}_{\text{E,wet}}}$  is the partial pressure of CO<sub>2</sub> in the equilibrator assuming 100% humidity where the gas is dried when it is measured inside the analyzer. It is necessary to correct the measured  $x\text{CO}_2$  values using the water vapor pressure (Pierrot *et al.*, 2009):

$$(p\text{CO}_2)_{\text{T}_{\text{E,wet}}} = x\text{CO}_2 [P_{\text{Eq}} - pH_2O] \quad (7)$$

where  $P_{\text{Eq}}$  is the pressure inside the equilibrator.  $pH_2O$  is the water vapor pressure over a seawater sample at the salinity and the temperature (K) of the equilibrator, and is given by (Pierrot *et al.*, 2009):

$$pH_2O = \exp[24.4543 - 67.4509(100/T) - 4.8489 \ln(T/100) - 0.000544 S] \quad (8)$$

In order to estimate the gas exchange at the sea surface, it is necessary to correct the  $(p\text{CO}_2)_{\text{T}_{\text{E}}}$  obtained to the measured sea surface temperature (DOE, 1994):

$$(p\text{CO}_2)_{\text{SST}} = (p\text{CO}_2)_{T_{\text{E,wet}}} \cdot \exp[0.0423(\text{SST} - T_{\text{E}})] \quad (9)$$

where SST is the sea surface temperature.

The  $f\text{CO}_2$  was computed from the calculated partial pressure of CO<sub>2</sub> ( $p\text{CO}_2$ ) values at in situ conditions, and corrected using the corresponding virial coefficients (DOE, 1994). That fugacity is given by:

$$(f\text{CO}_2)_{\text{SST}} = (p\text{CO}_2)_{\text{SST}} \cdot \exp \left[ \frac{(\text{B}(\text{CO}_2)_{\text{SST}} + 2(1 - x_{\text{CO}_2})^2 \cdot \delta(\text{CO}_2)_{\text{SST}})P_{\text{atm}}}{R \cdot \text{SST}} \right] \quad (10)$$

where SST is the in situ sea surface temperature (K),  $P_{\text{atm}}$  is the atmospheric pressure (atm),  $R$  is the gas constant ( $82.0578 \text{ cm}^3 \text{ atm mol}^{-1} \text{ K}^{-1}$ ),  $\text{B}(\text{CO}_2)_{\text{SST}}$  is the virial coefficient of pure carbon dioxide gas ( $\text{cm}^3 \text{ mol}^{-1}$ ) and  $\delta(\text{CO}_2)_{\text{SST}}$  is the virial coefficient of carbon dioxide in air ( $\text{cm}^3 \text{ mol}^{-1}$ ). The last two coefficients are given by:

$$\text{B}(\text{CO}_2)_{\text{SST}} = -1636.75 + 12.0408 \text{ SST} - 3.27957 \times 10^{-2} \text{ SST}^2 + 3.16528 \times 10^{-5} \text{ SST}^3 \quad (11)$$

$$\delta(\text{CO}_2)_{\text{SST}} = 57.7 - 0.118 \text{ SST} \quad (12)$$

### 3.3. Computational method

The vessel track between Cape Town and Durban is not exactly the same from the return (Durban-Cape Town) and the coastal processes are different (Fig. 1c). The data was separated into two sections, the Cape Town-Durban and Durban-Cape Town sections. In order to eliminate erroneous values due to poor measurements, data were manually de-spiked and all measurements with loss temperature and salinity were also deleted. As described by Pierrot *et al.* (2009), when temperature or salinity are missing for less than ½ h these values can be interpolated from another temperature or salinity, but in this highly variable region this is not appropriate. In order to simplify the presentation and calculations, data was averaged every 0.5°.

Since the seawater properties (SST, salinity and  $p\text{CO}_2$ ) change with the time in response to the solar heating cycle, climatological and atmospheric variations, all measurements were references to a single reference year (2009) in order to compute any seasonally related to the solar heating cycle and local physical forcing. All values measured were included into a reference 2009 year. Initially, this was done assuming concentrations of  $p\text{CO}_2$  between 2005 and 2012 have not changed. As described by González-Dávila *et al.* (2009), by fitting this monthly longitudinal degrees average data with a wave function the climatological cycles of SST and  $f\text{CO}_2$  can be obtained. The wave function is given by:

$$y = a + b(\sin 2\pi x) + c(\cos 2\pi x) + d(\sin 4\pi x) + e(\cos 4\pi x) \quad (13)$$

where  $y$  is SST or  $f\text{CO}_2$ ,  $x$  is the date (year fraction) and  $a$ ,  $b$ ,  $c$ ,  $d$  and  $e$  are the fitted constants, collected in the APPENDIX. In a second step and by fixing the seasonal values  $b$ ,  $c$ ,  $d$  and  $e$ , the interannual trend component  $f$  is computed:

$$y = a + f(x - 2005) + b(\sin 2\pi(x - 2005)) + c(\cos 2\pi(x - 2005)) + d(\sin 4\pi(x - 2005)) + e(\cos 4\pi(x - 2005)) \quad (14)$$

The normalization of the  $f\text{CO}_2$  values to the average value of sea surface temperature ( $T_{\text{mean}}$ ) in the three different regions allowed to remove the effects of the temperature on the observed  $f\text{CO}_2$ , following:

$$(f\text{CO}_2 \text{ at } T_{\text{mean}}) = f\text{CO}_2 \cdot \exp[0.0423(T_{\text{mean}} - T_{\text{obs}})] \quad (15)$$

## 4. Results

### 4.1. Hydrographic properties

Data was obtained from sixteen voyages made on different ships, between 2005 and 2012. For the purpose of describing the data variation, the experimental values have been plotted as a function of longitude or time.

**Table A.** Mean temperature (°C) grouped by season for the three regions, West Region (18°25'E–20°25'), South Region (20°75'E–29°25') and East Region (29°75'E–31°25'E).

Track	Region	Winter	Spring	Summer	Autumn
Cape Town	West	14.97	16.07	18.89	18.60
	South	17.28	18.07	21.04	25.16
Durban	East	20.56	22.19	25.08	25.34
	West	14.52	16.07	20.24	18.45
Durban	South	18.18	19.24	22.67	21.10
	East	20.68	22.55	25.97	25.49

The initial and de-spiked temperature measurements made during some representative voyages along the QUIMA-VOS line from Cape Town (33°55'S–18°25'E) to Durban (29°53'S–31°03'E) and return are plotted in Fig. 2. From the West to the East, the figure shows the values tend to increase in all seasons but there are also some significant variations. In the proximity of Cape Town (18°–19°E) and Port Alfred (26°E) different from the trends are clearly observed when the ship goes from Cape Town to Durban in its closest way to the shore. In the East Region, the temperature was more uniform during the winter and spring than in the rest of the seasons and regions. The minimum value recorded was 12.1°C around 18°75'E in November, the maximum recorded value was 27.3°C in February close to 30°75'E. Mean temperatures are presented in Table 1 distinguishing between the journeys to and from Durban. For the Cape Town-Durban vessel track, the mean temperature was  $20.3 \pm 3.6^\circ\text{C}$ , while in the returns track from

Durban the temperature was  $20.4 \pm 3.4^\circ\text{C}$ . During summer, the upwelling cell front near Cape Town showed a wide variation from  $4.0^\circ\text{C}$  (smaller change recorded in January 2011) to  $11.0^\circ\text{C}$  (grater change recorded in January 2007), the mean minimum was  $11.9^\circ\text{C}$  and the maximum was  $21.7^\circ\text{C}$  with an average difference of  $6.8^\circ\text{C}$ . Around Port Alfred, the SST gradient was more marked on the East than the West and from November to March than in the rest of the year. Maximum differences were around  $10^\circ\text{C}$  and minimum  $2.8^\circ\text{C}$ , on the West Region, where SST varied from  $18.6^\circ\text{C}$  (average minimum) to  $26.4^\circ\text{C}$  (average maximum).

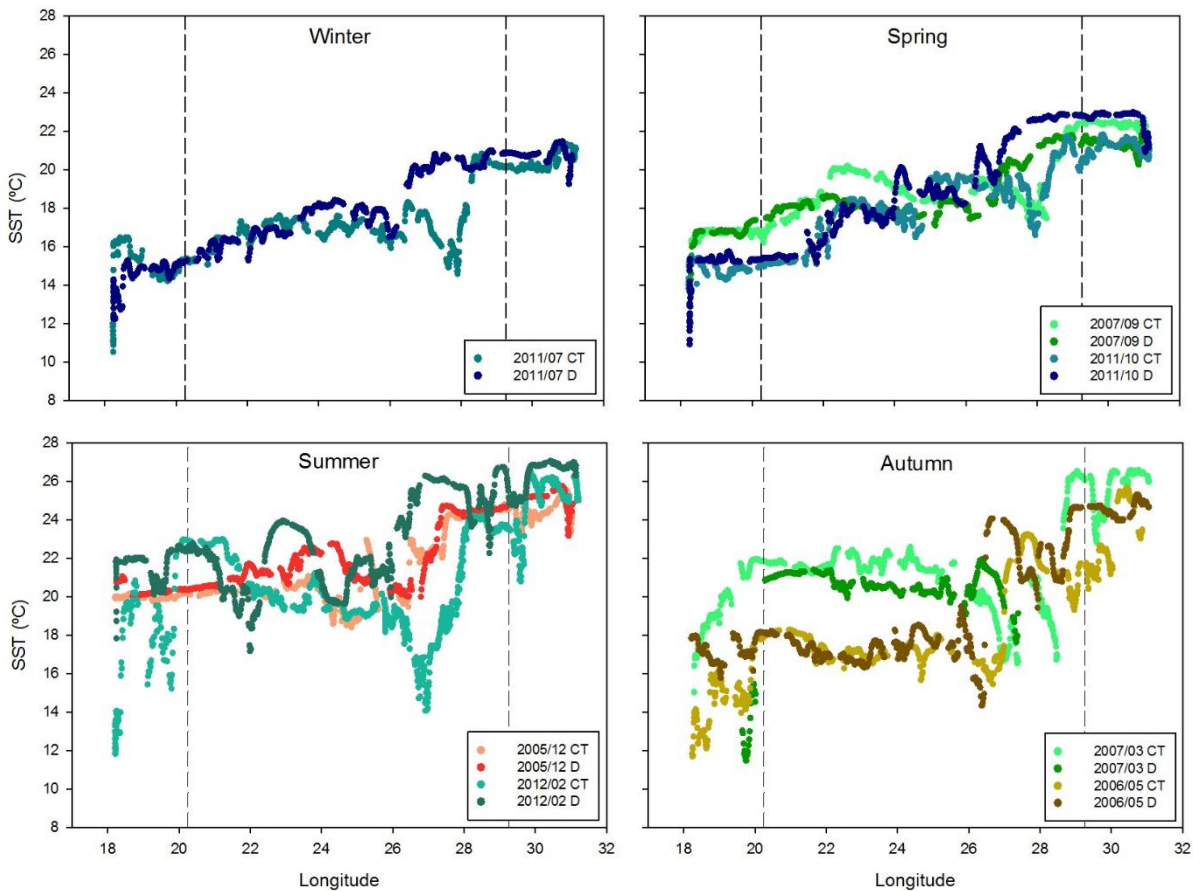


**Figure 2.** Sea surface temperature along the QUIMA-VOS line grouped by seasons. Dash line indicates the boundaries between the West and South Regions ( $20^\circ25'E$ ) and between South and East Regions ( $29^\circ25'E$ ).

The system also recorded salinity measurements presenting high variability along the coast. In Fig. 3, summer values are plotted from two voyages. 2005 values were more uniform than values from 2012 which show a relative wide dispersion close to Cape Town and Port Alfred, when values close to 34.5 were recorded in very narrow areas. Mean salinity does not differ too much between Cape Town – Durban and Durban – Cape Town tracks, being  $34.7 \pm 1.95$  and  $34.9 \pm 0.38$ , respectively. Values of about 35.2 were found near Port Alfred during summer and autumn, that also followed the lowest temperatures than for the surroundings, corresponding with SST from  $13^\circ\text{C}$  to  $17^\circ\text{C}$ . Near Durban,

salinities around 35.2 were found during summer and autumn travel but none had temperatures below 24°C.

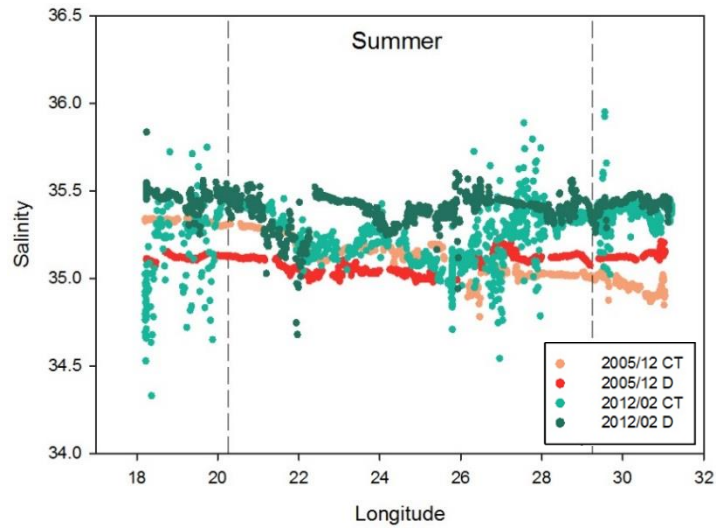


**Figure 3.** Sea surface salinity during summer along the QUIMA-VOS line representative for the studied area.

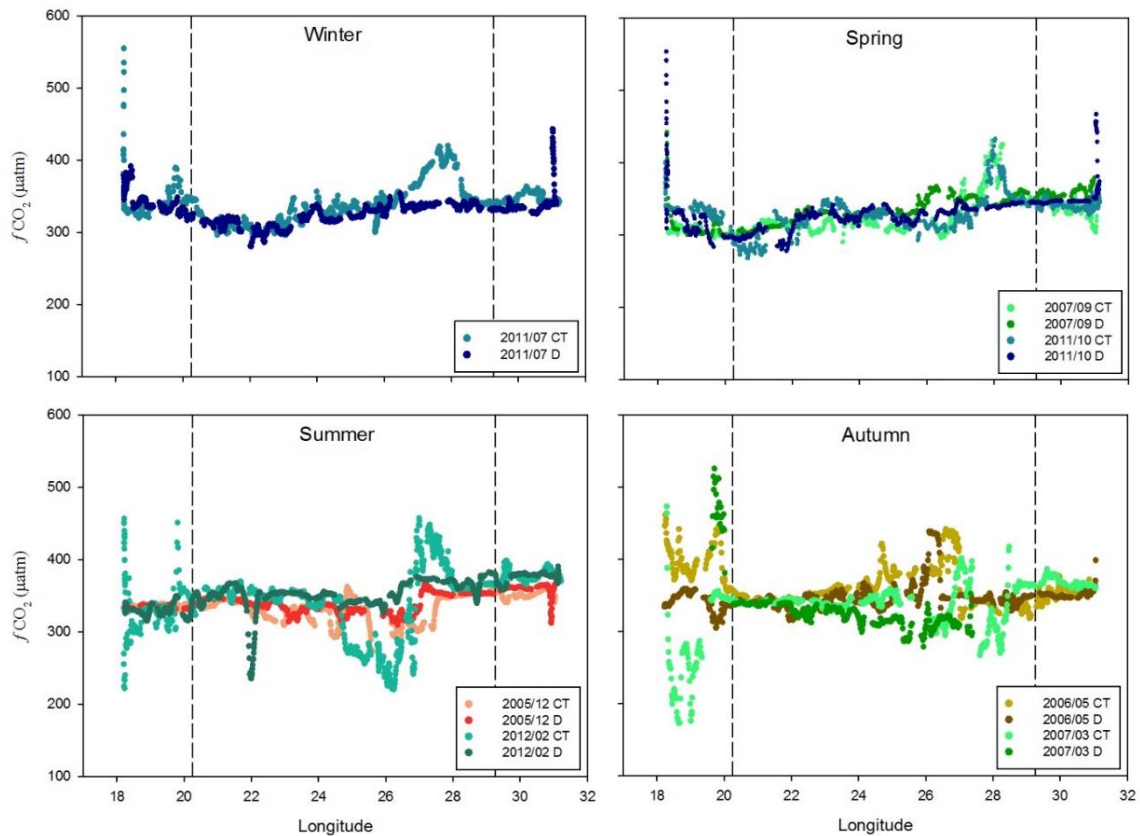


**Figure 4.** Representative  $f\text{CO}_2$  data grouped by seasons along the QUIMA-VOS line in South African Coastal region.

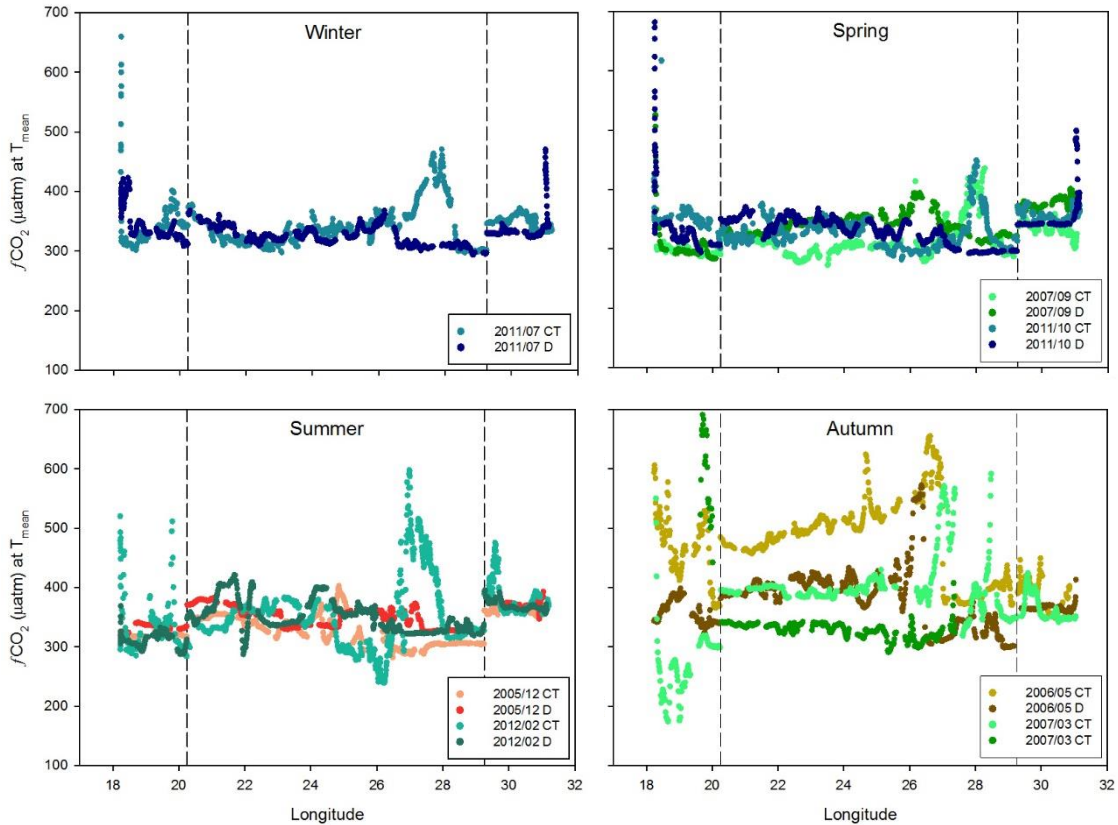


Figure 5. The  $f\text{CO}_2$  seasonal variations at mean temperature ( $T_{\text{mean}}$ ) along the QUIMA-VOS line.

## 4.2. Sea water $f\text{CO}_2$

The fugacity of carbon dioxide values calculated along the sixteen voyages from the sea surface water  $x\text{CO}_2$  measurement are plotted in Fig. 4 grouped by seasons and for the same cruises as those presented in Fig. 3. The  $f\text{CO}_2$  values for each season are relatively constant along the track in the range 300  $\mu\text{atm}$  to 380  $\mu\text{atm}$  throughout the year with important minimums and maximums centered around 18°E and 27°E. Values from 170  $\mu\text{atm}$  to 520  $\mu\text{atm}$  were recorded in the western region during autumn and between 220  $\mu\text{atm}$  and 460  $\mu\text{atm}$  during summer and autumn in the 25–28°E region.

The  $f\text{CO}_2$  pattern depends on the counteracting and seasonal variation effects controlled by thermodynamics, biology and air-sea gas exchange contribution. As described by Takahashi *et.al* (2002), to understand the relative importance of the temperature effect on the  $f\text{CO}_2$  seasonal changes the observed  $f\text{CO}_2$  value was normalized to a constant temperature using Eq. 9 ( $f\text{CO}_2$  instead of  $p\text{CO}_2$ ). The average temperatures used were those recorded in Table 1. Variations in the normalized quantity represent changes in the total  $\text{CO}_2$  concentrations due to physical and biological processes and are shown in Fig. 5. Values in the West Region were amplified while the effect in the East Region was less marked. The mean seawater  $f\text{CO}_2$  annual values obtained were

346.9±14.9 μatm for the Cape Town-Durban track and 355.9±17.2 μatm for the return. Autumn showed the most important changes varying from ~350 μatm to ~500 μatm.

The seasonal air-sea CO<sub>2</sub> gradients ( $\Delta f\text{CO}_2$ ) calculated from the difference of  $f\text{CO}_2$  between the seawater and the atmosphere integrated each 0.5° are plotted in Fig. 6. When both vessels tracks (single and return) are plotted, a significant difference is observed related to the different water properties recorded in each track. The mean atmospheric  $f\text{CO}_2$  recorded in the entire database was  $373.82 \pm 10.2 \mu\text{atm}$ . The deviation related to the seasonality of the atmospheric values, with maximum values of  $377.0 \pm 4.4 \mu\text{atm}$  in winter and minimum values of  $371.8 \pm 6.2 \mu\text{atm}$  in summer. Negative  $\Delta f\text{CO}_2$  values indicate CO<sub>2</sub> uptake by the ocean and dominated throughout the year with some source episodes close to 27°E, in the Port Alfred region. The average  $\Delta f\text{CO}_2$  value for the full period and region was  $-33.1 \pm 34.1 \mu\text{atm}$ . The most negative  $\Delta f\text{CO}_2$  value were observed during spring in the West (average value of  $-59.10 \pm 25.8 \mu\text{atm}$ ) and South Region (average value of  $-54.0 \pm 35.2 \mu\text{atm}$ ) in the Durban–Cape Town direction, while in the East Region they were observed during winter (average value of  $-43.5 \pm 19.8 \mu\text{atm}$ ) also in the Durban–Cape Town way.

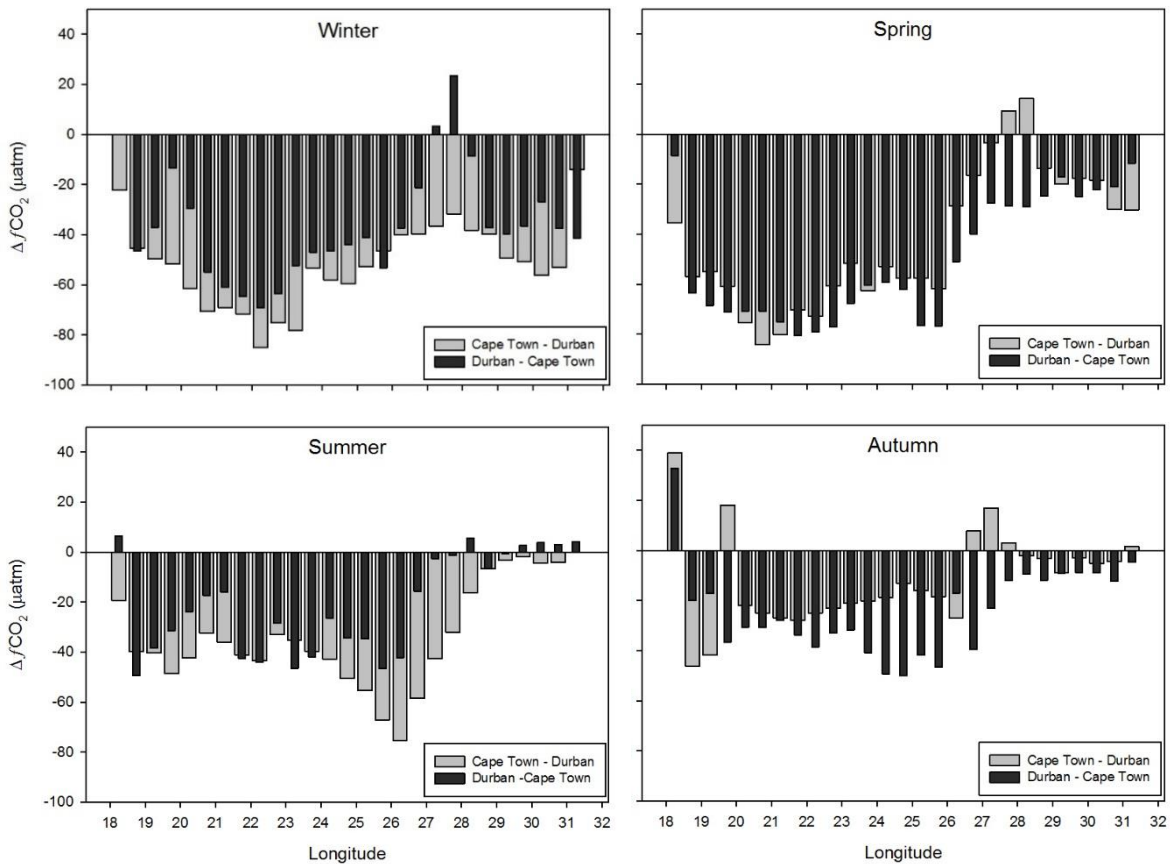


**Figure 6.** Seasonal average difference between seawater and atmospheric  $f\text{CO}_2$  ( $\Delta f\text{CO}_2 = f\text{CO}_{2,sw} - f\text{CO}_{2,atm}$ ). Different colors represent the vessel track.

### 4.3. Fits of harmonic time functions

Fig. 7 shows an example of seasonal variability and curve fit at 19°25'E longitude, in the West Region. Maximum temperatures were observed by the end of January while coolest observations corresponded to the end of August, during Austral winter. Fugacity peaks follow the inverse trend of temperature, where the maximum of  $f\text{CO}_2$  followed the minimum on SST. The dashed lines indicate the trends of interannual variations, negative slopes means that the parameter tend to decrease over time and positive slopes indicate that recent measurements are higher than previous ones. Slopes are recorded in Appendix tables (C and D). Along the entire South African QUIMA-VOS line SST trends were negative (Fig. 1b) while the seawater fugacity tend to increase through the years.

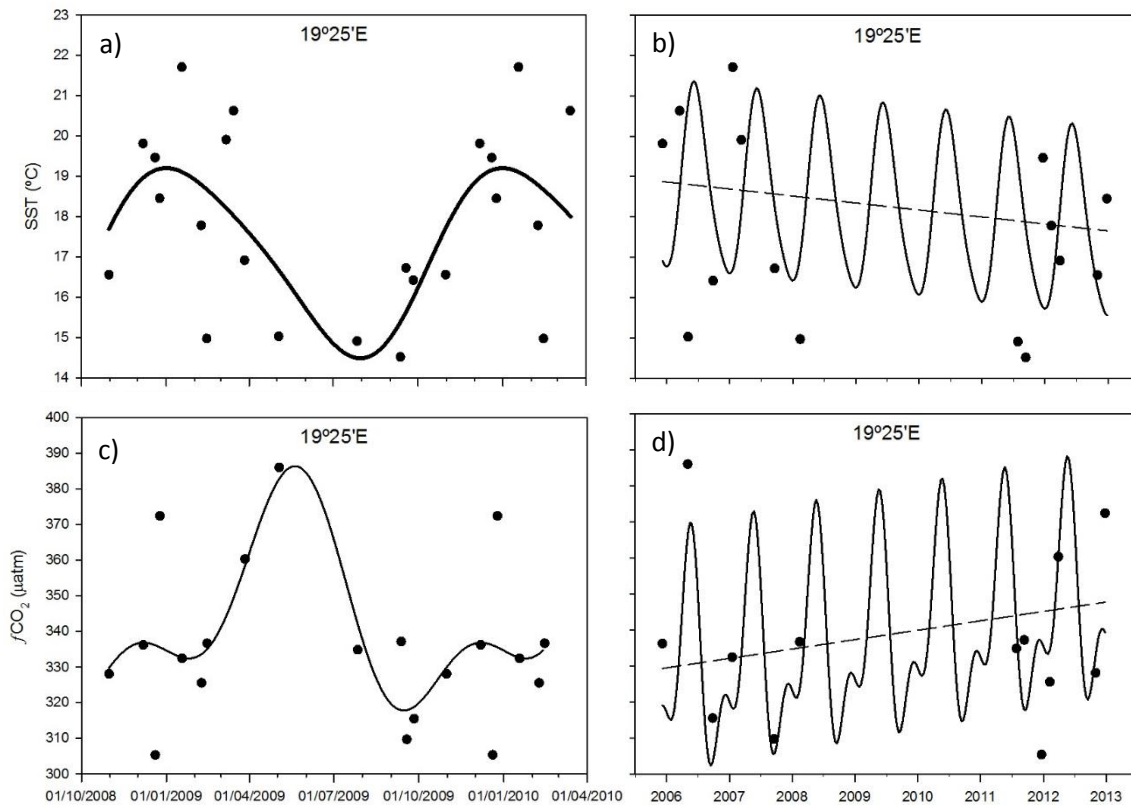


**Figure 7.** Seasonal cycle of 19°25'E location corresponding to Cape Town–Durban track. a) Sea surface temperature cycle obtained with fitting the Eq. 12 to average in situ measurement (dots) corrected to a single reference year (2009). b) Residuals between measured and seasonal detrended data (dashed line). Figures “c” and “d” are the same of “a” and “b” but in terms of carbon dioxide fugacity. The solid curve is a trend line obtained with parameters recorded in APPENDIX tables C and D.

## 5. Discussion

### 5.1. Hydrographic properties

SST increased from west to east showing the effect of the Benguela Current, Agulhas Current and filaments of coastal upwelled water in the three different locations. As described by González-Dávila (2009), near Cape Town the upwelling cells are seasonally affected by strong winds and show an important front during Austral summer (February). However, the increase in temperature in the front from this study (6.8°C) is greater than that described by the authors (4.5°C), due to the northern Atlantic track considered in their study, that provided lower temperature seawaters in the North Benguela Region. South West Indian Central Waters have temperature of about 13°C that may increase to 17°C due to upwelling mixing with surface water (South Indian Tropical Surface Water and South West Indian Subtropical Surface Water) (Lutjeharms *et al.*, 2000) which explains the values recorded around Port Alfred. Higher temperatures can be explained by the high stratification of waters. The difference between the Cape Town–Durban track and the return near 26°50'E indicates the presence or absence of coastal upwelling effects and, where it had not outcropped, temperatures greater than 22°C show the core of the Agulhas Current. Durban temperature minimum values coincided with South West Indian Central Water salinity referenced values but never with their temperature due to the high mixing with South Indian Tropical Surface Water. Salinities below 35.2 could be Antarctic Intermediate Water, according to Lutjeharms *et al.* (2000b). The upwelling is to be observed in South and East Regions through the year so the wind can not be the only factor that produce water outcrop, as described by Lutjeharms *et al.* (2000) and Lutjeharms *et al.* (2000b). The stability of East Region surface temperature is related to the Agulhas Current constancy, in fact it seems that the front is always in the same position (Fig. 2). This agrees with Krung and Tournadre (2012), whose study suggests that the Agulhas Current's core does not display annual cycles and the variations in path are dominated by passage of offshore meanders.

### 5.2. Fugacity of carbon dioxide

The study region presented a complex distribution of seawater CO<sub>2</sub> with saturated and low concentration areas. Higher and lower values over the mean are recorded around Cape Town, Port Alfred and Durban. Despite of this episodes the other values were always below atmospheric content (374  $\mu$ atm) as reported by González-Dávila for the west South African coast (2009), acting The South African coastal region, over an annual scale, as a sink of carbon dioxide.

West Region  $f\text{CO}_2$  maxima recorded during winter and spring are less pronounced in summer and autumn when important minima were also observed, as was the case during summer 2012 near 26°E (Fig. 4). These extreme values are consistent with temperature minima confirming the upwelling presence, where CO<sub>2</sub> rich waters outcrop forcing the system to act as a source. Systems dominated by upwelling dynamics generate an increase in  $f\text{CO}_2$  that can be overcompensated with the temperature decrease (16  $\mu\text{atm}/^\circ\text{C}$ ). Values under 300  $\mu\text{atm}$  in upwelling cells are also explained by the photosynthetic uptake of CO<sub>2</sub> using the nutrient provided during summer and also observed during autumn coinciding with the maximum runoff (James *et al.*, 2013) that could also provide nutrients. The CO<sub>2</sub> sink recorded in this coastal region agreed well with values reported in other marginal seas and coastal regions (Borges *et al.*, 2005; Cai and Dai, 2004; Chen *et al.*, 2013; Chen and Borges, 2009).

Temperature effects displayed in Fig. 5 over  $f\text{CO}_2$  show different patterns. The West Region fugacity accentuation is explained by the oceanographic conditions imposed by the upwelling cells. The same occurs in the East Region but less marked probably due to the higher temperatures. Variation near Port Alfred in summer 2012 (Cape Town–Durban track) showed two different patterns, a weakening of the minimum and an accentuation of the maximum. The decrease of fugacity is due to the biological utilization of CO<sub>2</sub> that force the system to act as a sink. In the other hand, maximum values are related to an increase in the upwelling strength with a new water outcropped. Wide variation in the South Region is showed during autumn. The temperature effect over this region explains the increase of  $\sim 100 \mu\text{atm}$  (Fig. 5, autumn) but the rest of the variance was due to the oceanic conditions.

In accordance with Chen *et al.* (2013), water over the continental shelf presented a lower concentration of CO<sub>2</sub> than in the open ocean. Carbon dioxide uptake dominated all year around as displayed in Fig. 6 with isolated locations where the coastal water acted as a source. This region acts as an active sink due to carbon consumption by phytoplankton. Positive  $\Delta f\text{CO}_2$  values were concentrated near Cape Town, Port Alfred and only in summer near Durban coinciding with the location of upwelling cells. The Figure do not show a clear seasonality as described by Lutjeharms *et al.* (2000) for the southern coast, indicating the important changes in the area considered. Only in the western region, CO<sub>2</sub> seawater concentration showed a peak in summer producing positive  $\Delta f\text{CO}_2$  values as suggested by Veitch *et al.* (2010).

### 5.3. Trends of carbon dioxide

The fugacity of CO<sub>2</sub> along VOS line not show a homogeneous global seasonal variability but over the single 0.5°, a minimum during winter and a variable maximum

during summer and spring appears (Fig. 7c). The annual cycles shown in temperature and fugacity (Fig. 7a, 7c) across 19°25'E were consistent with the climatological variation of coastal South Africa. Maximum wind blows during summer (Veitch *et al.*, 2010) producing water outcrop that leads to surface temperature decreases and increases in fugacity of carbon dioxide. Harmonic curves do not differ too much between the different longitudinal approximations, excluding fits on upwelling cells which present a greater variability.

From 2005 to 2012, the temperature decreased for all longitudes and the fugacity increased. It does not coincide with the trends found by González-Dávila *et al.* (2009) in the South Benguela Region, north of 33°S where temperature and fugacity decreased between 2005 and 2008. However, as described by Rouault *et al.* (2009) for the southern and eastern African areas, higher atmospheric temperatures over the Indian Ocean could increase the Agulhas Current temperature whilst the strength of south-easterly and easterly winds increase the upwelling favorable conditions. These coupled effect could explain the negative and positive trend of SST and  $f\text{CO}_2$  presented in this study, confirming the reinforcing of the upwelling conditions in the South African coastal region.

#### **5.4. Limitation and future directions**

In coastal studies temporal resolution is always a limiting factor due to the high variability of coastal processes. In order to clearly define seasonal and interannual trends of carbon dioxide longer time series of data are required.

The advantages of using an automated underway xCO<sub>2</sub> system have been presented: regular observations of seawater when the vessel track is spatially and temporally stable, rapid response time of the equilibrator, high precision, low equipment maintenance and lower cost. However, the study success is affected by: unsteady vessel track, inlet of water contaminated from port activities and system failures away from home port.

The next step in this research line will be the calculation of the air-sea exchange of CO<sub>2</sub> using wind data obtained by in situ or satellite measurements and the role of this coastal region in global carbon budgets

## **6. Conclusion**

The South African coastal region presents a complex surface hydrographic system that includes boundary currents, upwelling cells, fronts and filaments which affect the biogeochemical properties of sea water. Three regions were affected by different coastal

process and relates temperature distribution. The fugacity of carbon dioxide was measured along the QUIMA-VOS line from 18°25'E (Cape Town) to 31°25'E (Durban). From 2005 to 2012 sea surface water highlighted the ocean uptake of carbon dioxide over the continental shelf with a mean gradient of -33.1  $\mu\text{atm}$ . The area does not present a clear seasonality due to the presence all year around of upwelling cells in the southern region. Maximum sink values were recorded during spring (-59.1 $\pm$ 25.8  $\mu\text{atm}$ ). Hydrographic conditions were the major factor that controls the concentration of sea water carbon dioxide while the primary production uptake of dissolved CO<sub>2</sub> favored low  $f\text{CO}_2$  values for the area.

Comparison of  $f\text{CO}_2$  results over 6 years of data showed a clear seasonal and interannual variability. Seasonality of the Agulhas Current and easterly winds are the main causes of the observed variability over surface water. Maximum carbon dioxide fugacity coincided with minimum temperatures during austral summer, when wind-driven upwelling dominate the region, and strong  $f\text{CO}_2$  anomalies are correlated with SST anomalies. The interannual variability observed in temperature and fugacity indicate inverse trends. SST decreased with time while  $f\text{CO}_2$  increase as response to the heating of Agulhas Current and the intensification of the winds. Longer time series of data are required in order to establish the seasonal and interannual variability in a more reliable way.

## **Acknowledgments**

The *Universidad de Las Palmas de Gran Canaria* is acknowledged for giving me the opportunity to perform this work. Thanks goes also to the Marine Science Faculty for supporting students in their education curriculum and to the QUIMA research group for taking me in their team and giving me the opportunity to gain experience in this research work.

I would like to thank my supervisors, Prof. Dr. Melchor González Dávila and Prof. Dr. J. Magdalena Santana Casiano, for sharing their knowledge and guiding me through the process of developing this study.

## References

- Bates N.R., Astor Y.M., Church M.J., Currie K., Dore J.E., González-Dávila M., Lorenzoni L., Muller-Karger F., Olafsson J. and Santana-Casiano J.M. (2014): A time-series view of changing ocean chemistry due to ocean uptake of anthropogenic CO<sub>2</sub> and ocean acidification. *Oceanography* 27(1), 126–141.
- Beal L.M., De Ruijter W.P.M., Biastoch A., Zahn R. and SCOR/WCRP/IAPSO Working Group 136 (2011): On the role of the Agulhas system in ocean circulation and climate. *Nature*, Vol. 472, 429-435.
- Biastoch A., Reason J.C., Lutjeharms J.R.E. and Boebell O. (1999): The importance of flow in the Mozambique Channel to seasonality in the greater Agulhas Current system. *Geophysical Research Letters*, Vol. 26, No. 21, 3321-3324.
- Borges A. V., Delille B., and Frankignoulle M. (2005): Budgeting sinks and sources of CO<sub>2</sub> in the coastal ocean: Diversity of ecosystems counts, *Geophys. Res. Lett.*, 32, L14601, doi:10.1029/2005GL023053.
- Cai W. and Dai M. (2004): Comment on “Enhanced Open Ocean Storage of CO<sub>2</sub> from Shelf Sea Pumping. *Science* 306, 1477.
- Chen C.T.A., Huang T.H., Chen Y.C., Bai Y. He X. and Kang Y. (2013): Air-sea exchanges of CO<sub>2</sub> in the world’s coastal seas. *Biogeosciences*, 10, 6509-6544, doi:10.5194/bg-10-6509-2013.
- Chen C.T.A. and Borges A.V. (2009): Reconciling opposing views in the carbon cycling in the coastal ocean. Continental shelves as sinks and near-shore ecosystems as sources of atmospheric CO<sub>2</sub>. *Deep-Sea Research II*, 56, 578–590, doi:10.1016/j.dsr2.2009.01.001.
- DOE (1994): Handbook of methods for the analysis of the various parameters of the carbon dioxide system in sea water; version 2. A. G. Dickson & C. Goyet, eds., ORNL/CDIAC-74.
- Doney S.C., Fabry V.J., Feely R.A. and Kleypas J.A. (2009): Ocean Acidification. The Other CO<sub>2</sub> Problem. *Annual Review of Marine Science*. 1:169-92, doi:10.1146/annurev.marine.010908.163834.
- González-Dávila M., Santana-Casiano J.M. and Ucha I.R (2009): Seasonal variability of *f*CO<sub>2</sub> in the Angola-Benguela region. *Progress in Oceanography* 83, 124-133.

Gruber, N., et al. (2009), Oceanic sources, sinks, and transport of atmospheric CO<sub>2</sub>, *Global Biogeochem. Cycles*, 23, GB1005, doi:10.1029/2008GB003349.

Herr, D. and Galland, G.R. (2009): *The Ocean and Climate Change. Tools and Guidelines for Action*. IUCN, Gland, Switzerland. 72 pp.

James N.C., Van Niekerk L., Whitfield A.K., Potts W.M., Götz A., Paterson A.W. (2013): Effects of climate change on South African estuaries and associated fish species. *Climate Research*, Vol. 57, 233–248.

Key R.M, Kozyr A., Sabine C. L., Lee K., Wanninkhof R., Bullister R.L., Feely R. A., Millero F. J., Mordy C., and Peng T.H. (2004): A global ocean carbon climatology: Results from Global Data Analysis Project (GLODAP). *GLOBAL BIOGEOCHEMICAL CYCLES*, VOL. 18, doi: 10.1029/2004GB002247.

Krug M. and Tournadre J. (2012): Satellite observations of an annual cycle in the Agulhas Current. *Geophysical Research Letter*, 39, L15607, doi:10.1029/2012GL052335.

Le Quéré C. *et al.*, (2015): Global carbón Budget 2014. *Earth System Science Data*, 7, 47–85.

Lutjeharms J.R.E., Cooper J. and Roberts M. (2000): Upwelling at the inshore edge of the Agulhas Current. *Continental Shelf Research* 20, 737-761.

Lutjeharms J.R.E., Valentine H.R. and Van Ballegooyen R.C. (2000b): The hydrography and water masses of the Natal Bight, South Africa. *Continental Shelf Research* 20, 1907-1939.

Orr J.C. *et al.*, (2005): Anthropogenic ocean acidification over the twenty-first century and its impact on calcifying organisms. *Nature* 437, doi:10.1038/nature04095.

Pierrot D., Neill G., Sullivan K., Castle R., Wanninkhof R., Lüger H., Johannessen T., Olsen A., Feely R.A. and Cosca C.E. (2009): Recommendations for autonomous underway pCO<sub>2</sub> measuring systems and data-reduction routines. *Deep-Sea Research II* 56, 512–522.

Rouault M., Pohl B. and Penven P. (2010): Coastal oceanic climate change and variability from 1982 to 2009 around South Africa. *African Journal of Marine Science*, 32:2, 237-246, doi:10.2989/1814232X.2010.501563.

Sabine C. L. *et al.*, (2004): The ocean sink for anthropogenic CO<sub>2</sub>. *Science* 305, 367–370.

Santana-Casiano J.M., González-Dávila M. and Ucha I.R. (2009): Carbon dioxide fluxes in the Benguela upwelling system during winter and spring: A comparison between 2005 and 2006. *Deep-Sea Research II* 56, 533–541.

Sarmiento J.L. and Gruber N. (2002): Sinks of anthropogenic carbon. *Physics Today* 55, 30-36.

Slegenthaler U. and Sarmiento J.L. (1993): Atmospheric carbon dioxide and the ocean. *Nature* 365, 119-125.

Takahashi T., Sutherland S.C., Sweeney C., Poisson A., Metzl N., Tilbrook B., Bates N., Wanninkhof R., Feely R.A., Sabine C., Olafsson J. and Nojiri Y. (2002): Global sea–air CO<sub>2</sub> flux based on climatological surface ocean *p*CO<sub>2</sub>, and seasonal biological and temperature effects. *Deep Sea Research Part II* 49, 1601-1622.

Veich J., Penven V. and Shillington F. (2010): Modeling equilibrium dynamics of the Benguela Current System. *Journal of Physical Oceanography*, Vol. 40, 142-164, doi:10.1175/2010jpo4382.1

CO<sub>2</sub> FLUXES IN THE SOUTH AFRICAN COASTAL REGION

Appendix

**Table A.** Results of harmonic curve fits (Eq. 7) for SST (°C) in 0.5 degrees resolution. Listing longitude (°E), the coefficients (a, b, c, d and e), the standard error (°C) and coefficient of determination (R<sup>2</sup>). On the left results of Cape Town – Durban track against the back (Durban – Cape Town) on the right.

Longitude	a	b	c	d	e	Standard error	R <sup>2</sup>	Longitude	a	b	c	d	e	Standard error	R <sup>2</sup>
18°25'	15.60	-0.03	1.24	-0.54	-0.15	2.54	0.31	18°25'	15.88	1.37	0.85	-0.66	0.89	3.24	0.22
18°75'	17.30	0.86	2.14	-0.14	-0.05	2.18	0.33	18°75'	17.65	1.86	1.78	-0.28	-0.07	1.87	0.55
19°25'	16.96	0.68	2.18	-0.32	0.06	1.99	0.38	19°25'	18.12	1.87	2.39	-0.05	0.17	1.36	0.77
19°75'	17.38	0.87	2.53	-0.83	0.04	2.26	0.41	19°75'	17.83	0.50	2.53	0.42	1.62	2.25	0.57
20°25'	18.35	1.94	2.79	0.13	0.04	0.97	0.87	20°25'	18.62	2.08	2.89	0.51	0.06	0.65	0.95
20°75'	18.50	1.81	2.82	0.33	0.10	0.79	0.91	20°75'	18.79	2.04	2.74	0.63	0.05	0.69	0.95
21°25'	18.70	1.53	2.38	0.21	0.41	0.95	0.85	21°25'	18.70	1.65	2.57	0.77	0.27	1.06	0.86
21°75'	18.67	1.38	2.13	0.21	0.18	1.13	0.74	21°75'	18.68	1.43	2.25	0.56	0.38	1.31	0.75
22°25'	18.50	0.95	1.80	0.44	0.13	1.55	0.50	22°25'	18.66	1.18	1.86	0.75	0.48	1.61	0.62
22°75'	18.93	0.80	1.61	0.63	0.62	1.36	0.59	22°75'	18.83	1.15	2.35	1.67	0.43	1.20	0.84
23°25'	18.79	0.64	1.49	0.42	0.57	1.49	0.49	23°25'	18.97	1.26	2.50	1.22	0.50	1.32	0.79
23°75'	18.81	0.60	1.62	0.37	0.45	1.32	0.54	23°75'	19.40	1.21	1.98	0.80	0.95	0.95	0.85
24°25'	18.49	0.91	1.52	0.67	0.28	1.28	0.59	24°25'	19.55	0.72	1.81	0.20	1.06	1.56	0.55
24°75'	18.30	0.84	1.46	0.70	0.23	1.13	0.62	24°75'	19.58	0.83	1.94	0.10	1.00	1.19	0.69
25°25'	18.76	0.65	1.16	0.34	0.35	1.22	0.47	25°25'	19.30	1.22	1.89	0.76	0.37	1.06	0.79
25°75'	18.27	0.71	1.36	0.89	0.21	1.27	0.55	25°75'	19.18	0.70	1.51	0.58	0.37	1.44	0.53
26°25'	18.25	0.40	1.06	0.81	0.37	2.43	0.18	26°25'	18.96	0.96	2.47	1.05	-0.19	1.94	0.54
26°75'	18.23	0.15	-0.01	0.27	1.21	2.98	0.10	26°75'	21.17	1.94	-0.63	-0.02	1.13	2.18	0.45
27°25'	18.88	1.11	-0.55	-0.15	1.55	2.72	0.17	27°25'	22.04	0.86	1.33	0.57	0.05	2.57	0.21
27°75'	19.26	1.52	0.57	-0.49	1.84	2.82	0.32	27°75'	22.47	1.53	2.46	0.65	-1.67	1.86	0.55
28°25'	20.68	0.95	1.16	0.57	2.03	1.45	0.72	28°25'	22.53	1.45	2.19	0.19	-1.88	1.89	0.48
28°75'	22.39	1.48	1.97	0.85	0.58	1.30	0.73	28°75'	23.28	1.52	2.10	-0.09	-0.69	0.62	0.88
29°25'	22.66	1.48	2.67	0.57	-0.55	1.28	0.73	29°25'	23.72	2.09	1.63	-0.38	-0.28	0.78	0.85
29°75'	22.64	1.46	2.00	0.56	-0.49	1.02	0.75	29°75'	23.78	2.08	1.88	-0.21	-0.40	0.62	0.91
30°25'	23.54	2.09	1.34	-0.59	0.07	1.01	0.75	30°25'	23.84	2.10	2.30	-0.12	-0.44	0.50	0.95
30°75'	23.83	1.86	1.91	-0.13	0.00	0.52	0.93	30°75'	24.06	2.21	1.88	-0.09	0.10	0.62	0.94
31°25'	23.36	1.76	1.90	0.31	-0.18	0.49	0.94	31°25'	23.64	2.38	1.97	-0.19	-0.29	0.29	0.98

CO<sub>2</sub> FLUXES IN THE SOUTH AFRICAN COASTAL REGION

**Table B.** Results of harmonic curve fits (Eq. 7) for  $f\text{CO}_2$  ( $\mu\text{atm}$ ) in 0.5 degrees resolution. Listing longitude ( $^{\circ}\text{E}$ ), the coefficients (a, b, c, d and e), the standard error ( $\mu\text{atm}$ ) and coefficient of determination ( $R^2$ ). On the left results of Cape Town – Durban track against the back (Durban – Cape Town) on the right.

Longitude	a	b	c	d	e	Standard error	R <sup>2</sup>	Longitude	a	b	c	d	e	Standard error	R <sup>2</sup>
18°25'	376.60	37.00	-28.86	-21.96	-1.19	58.77	0.18	18°25'	379.58	19.79	2.43	7.43	-15.65	68.73	0.09
18°75'	340.61	12.90	-19.88	-18.2	15.96	30.62	0.2	18°75'	336.22	12.28	-19.49	-12.98	12.95	15.59	0.52
19°25'	342.47	12.28	-20.56	-16.89	14.78	27.67	0.24	19°25'	336.55	19.62	-13.82	-7.88	10.04	12.19	0.70
19°75'	356.40	36.91	-35.77	-24.64	4.05	29.82	0.49	19°75'	336.29	40.07	5.33	-5.87	-15.30	41.45	0.42
20°25'	333.93	24.18	-8.85	-7.39	6.54	25.63	0.31	20°25'	331.44	18.48	4.79	-1.17	8.67	6.54	0.90
20°75'	328.84	27.97	5.39	-7.27	7.40	17.96	0.62	20°75'	331.41	19.02	9.29	0.31	8.27	5.53	0.94
21°25'	328.04	20.84	3.70	-13.48	10.77	20.76	0.49	21°25'	331.43	20.49	4.21	6.87	7.80	11.29	0.82
21°75'	327.26	15.69	2.58	-10.10	6.17	25.50	0.24	21°75'	324.18	15.80	-3.45	-6.13	11.45	21.24	0.35
22°25'	326.86	16.66	-1.13	-13.24	10.4	27.61	0.26	22°25'	319.60	11.55	-8.11	5.169	7.411	28.41	0.19
22°75'	333.85	16.94	5.42	-7.98	2.93	16.73	0.41	22°75'	324.88	14.35	-6.29	15.38	4.77	25.61	0.42
23°25'	339.63	12.21	-2.52	-11.61	4.63	18.23	0.26	23°25'	324.30	10.95	-8.79	-0.63	2.77	30.16	0.11
23°75'	337.21	17.30	-11.31	-7.43	10.91	18.04	0.36	23°75'	331.90	2.70	-8.17	-5.64	16.07	23.72	0.16
24°25'	339.64	13.49	-6.93	-13.56	2.94	22.02	0.19	24°25'	331.15	4.56	-2.26	5.71	14.18	18.99	0.32
24°75'	341.32	18.19	-23.75	-20.57	11.28	20.67	0.42	24°75'	325.28	2.01	-3.12	11.33	7.76	22.84	0.22
25°25'	341.07	15.02	-29.21	-28.48	16.40	24.96	0.45	25°25'	329.82	7.74	-17.43	11.32	16.80	23.12	0.38
25°75'	332.48	18.05	-29.89	-18.34	9.90	30.91	0.27	25°75'	330.08	1.79	-28.48	9.075	20.54	30.55	0.24
26°25'	342.28	1.48	-28.12	-47.53	-1.05	38.78	0.50	26°25'	347.078	3.07	-37.69	3.25	7.09	36.09	0.22
26°75'	362.03	13.38	-23.21	-44.07	-16.83	50.08	0.36	26°75'	336.89	-11.69	-0.82	32.24	-7.13	39.99	0.24
27°25'	360.73	2.65	7.14	-9.05	-40.42	62.06	0.20	27°25'	349.856	-0.65	11.71	3.58	6.15	17.42	0.25
27°75'	374.14	-8.45	-8.084	-9.27	-26.80	53.00	0.20	27°75'	356.81	8.96	16.35	1.95	6.22	14.89	0.53
28°25'	367.34	-10.66	11.39	1.98	-28.70	29.38	0.32	28°25'	356.94	10.61	17.66	-0.95	6.76	18.33	0.46
28°75'	356.67	0.46	20.39	-4.12	-11.44	16.41	0.29	28°75'	351.36	6.82	15.22	2.84	-6.58	5.08	0.81
29°25'	351.77	2.3	19.20	3.81	-5.94	9.90	0.53	29°25'	353.94	5.23	17.88	3.46	-8.46	8.44	0.62
29°75'	357.37	4.78	17.55	-0.91	-4.57	14.07	0.32	29°75'	354.30	9.35	16.90	1.48	-3.16	3.04	0.94
30°25'	358.75	4.32	13.36	0.39	-3.99	16.42	0.19	30°25'	354.03	8.33	19.45	1.58	-5.09	4.17	0.90
30°75'	356.08	13.07	9.98	-0.89	2.82	7.58	0.73	30°75'	356.11	8.47	16.76	2.97	-7.76	4.22	0.89
31°25'	354.85	14.63	8.74	-1.92	-0.72	12.74	0.52	31°25'	372.17	0.01	-1.30	7.05	-0.62	5.18	0.60

CO<sub>2</sub> FLUXES IN THE SOUTH AFRICAN COASTAL REGION

**Table C.** SST inteannual coefficients estimated with Eq. 14. On the left results of Cape Town – Durban track against the back (Durban – Cape Town) on the right.

Longitude	a	f	a	f
18°25'	17.60	-0.42	16.25	-0.08
18°75'	17.40	-0.02	17.19	0.09
19°25'	19.06	-0.17	19.89	-0.19
19°75'	17.79	-0.07	17.25	0.18
20°25'	18.08	0.08	18.74	-0.03
20°75'	19.68	0.13	19.10	-0.08
21°25'	18.49	0.06	19.33	-0.20
21°75'	18.60	0.02	19.52	-0.21
22°25'	19.68	-0.27	19.69	-0.26
22°75'	19.58	-0.09	19.13	-0.06
23°25'	19.38	-0.11	19.23	-0.06
23°75'	19.31	-0.09	19.78	-0.10
24°25'	19.03	2.05	20.10	-0.11
24°75'	18.83	-0.10	19.48	0.04
25°25'	19.66	-0.17	19.61	-0.04
25°75'	19.00	-0.14	19.83	-0.14
26°25'	19.42	-0.19	19.05	0.02
26°75'	20.31	-0.38	21.42	-0.03
27°25'	30.57	-0.16	22.34	-0.03
27°75'	22.12	-0.56	22.72	-0.07
28°25'	21.63	-0.20	23.14	-0.15
28°75'	23.10	-0.12	23.31	-0.02
29°25'	23.59	-0.15	23.42	-0.01
29°75'	22.82	-0.08	23.83	0.00
30°25'	23.55	0.01	23.67	0.06
30°75'	24.08	-0.05	23.50	0.09
31°25'	23.45	-0.02	23.73	-0.02

**Table D.** fCO<sub>2</sub> inteannual coefficients estimated with Eq. 14. On the left results of Cape Town – Durban track against the return (Durban – Cape Town) on the right

Longitude	a	f	a	f
18°25'	343.50	7.85	353.40	5.14
18°75'	330.23	1.94	329.28	1.56
19°25'	324.97	3.05	333.26	0.69
19°75'	344.26	2.69	342.01	-2.05
20°25'	329.97	0.74	332.19	-0.22
20°75'	320.81	1.63	334.78	-0.79
21°25'	320.38	1.82	336.46	-1.28
21°75'	316.56	2.01	328.78	-1.10
22°25'	330.45	-2.19	334.08	-3.48
22°75'	331.49	-1.71	337.28	-3.09
23°25'	320.85	4.03	327.87	-0.81
23°75'	327.37	2.38	324.99	1.83
24°25'	327.03	2.50	328.22	0.93
24°75'	341.83	0.27	330.51	-1.00
25°25'	348.26	-0.97	341.23	-2.78
25°75'	338.56	-0.67	338.87	-2.07
26°25'	330.65	2.18	372.03	-6.41
26°75'	342.08	3.19	372.44	-9.30
27°25'	328.92	6.71	351.59	0.11
27°75'	342.82	5.27	350.03	1.60
28°25'	358.65	2.62	348.94	1.86
28°75'	346.53	1.75	350.55	0.16
29°25'	346.04	1.25	359.84	-1.18
29°75'	349.20	1.81	353.14	0.29
30°25'	348.53	1.87	351.34	0.63
30°75'	348.29	1.58	356.30	-0.03
31°25'	338.08	3.06	372.44	0.00

## MEMORIA FINAL DEL TRABAJO DE FIN DE GRADO

### 1. Descripción de las actividades desarrolladas durante la realización del Trabajo de Fin de Grado

El Trabajo de Fin de Grado (TFG) se ha desarrollado en relación con las Prácticas Externas realizadas en el grupo de investigación QUIMA, bajo la supervisión del Dr. Melchor González Dávila y la Dra. J. Magdalena Santana Casiano, en la Universidad de Las Palmas de Gran Canaria (ULPGC).

Tras el tratamiento de datos recogidos a través de *Voluntary Observing Ships* (VOS) que operaron a lo largo de la QUIMA-VOS line se procedió a:

- Búsqueda bibliográfica. Para llevar a cabo la consulta se emplearon los recursos telemáticos y en papel proporcionados por la Biblioteca Universitaria de la ULPGC. Para la búsqueda de artículos científicos se consultaron diferentes bases de datos bibliográficas online a las que la Biblioteca Universitaria está adscrita, entre ellas destaca: *SCOPUS*, *Web of Science*, *Royal Society of Chemistry* y *Science Direct*.
- Formación en el estudio del sistema del dióxido de carbono. La realización del trabajo seleccionado supone un paso más en mi formación docente realizada en las asignaturas de Química Marina y Oceanografía Química, por lo que durante todo el periodo de trabajo he tenido que leer y profundizar, justo con mis tutores, en el tratamiento de datos del sistema del dióxido de carbono.
- Discusión de la información. Dado que el tratamiento de datos y la elaboración de gráficos fue realizada durante el desarrollo de las Prácticas externas se realizó directamente la discusión de la información recopilada.
- Instalación de equipos. Con el objetivo comprender el funcionamiento del sistema utilizado para la obtención de la información durante dos jornadas, 28 de Marzo y 3 de Mayo, la estudiante colaboró en el proceso de instalación de los equipos automatizados de medición de xCO<sub>2</sub> en el buque mercante (porta-contenedores) MARIANNA, perteneciente a la naviera MSC (Mediterranean Shipping Company). Durante la tarde del primer día las actividades a bordo del buque consistieron en: el análisis de la estructura del propio buque, con el fin de establecer el punto más idóneo para montar los equipos; iniciar el cableado necesario para conectar los dispositivos con la toma de aire atmosférico y el GPS. A lo largo de la segunda jornada se finalizó la instalación de los equipos,

terminando el cableado que vincula los diferentes mecanismos y conectando los distintos componentes.

## **2. Formación recibida**

Para el correcto desarrollo y representación de la información la alumna ha precisado incrementa sus habilidades y conocimientos en los siguientes programas informáticos:

- *Microsoft Excel.* Programa del paquete Office utilización de MACROS específicos elaborados para el estudio de parámetros químicos del océano.
- *SigmaPlot.* Software estadístico y gráfico utilizado para el procesamiento y representación de la información.
- *Underway xCO<sub>2</sub> system.* Equipos automatizados de medición de xCO<sub>2</sub> mediante los que se obtiene la información tratada en el presente estudio. El aprendizaje consistió en comprender el funcionamiento de los equipos y participar en su instalación.

## **3. Nivel de integración e implicación dentro del departamento y relaciones con el personal**

En las diferentes actividades desarrolladas durante los meses de trabajo en el seno del grupo de investigación la alumna se vio involucrada en diferentes ambientes y grupos de trabajo, con diferentes integrantes y funciones. La interacción en el interior de dichos equipos ha sido muy productiva debido no sólo a la diversidad formativa de los componentes sino del buen ambiente establecido. Estas relaciones sociales han amenizado y enriquecido la tarea de la estudiante.

## **4. Aspectos positivos y negativos más significativos en el desarrollo del TFT**

Los aspectos positivos más destacables son la adquisición de nuevos conocimientos y la posibilidad de afianzar los previamente adquiridos a lo largo del Grado.

## **5. Valoración personal del aprendizaje conseguido a lo largo del TFT**

Los conocimientos adquiridos durante el desarrollo del trabajo han permitido ampliar los conocimientos de la oceanografía química, en especial de la importancia de las regiones costeras dentro del ciclo carbono así como su papel en el cambio climático. Al mismo tiempo se hizo patente la importancia de los estudios interdisciplinarios en la dinámica oceánica.

Lo más importante en el desarrollo del trabajo fue entender lo que realmente hay detrás de un proyecto de investigación partiendo de las necesidades económicas, los acuerdos con empresas y grupos de investigación, atravesando etapas formativas cada vez más específica, aprendiendo sobre protocolos y tomas de muestras para finalizar con la necesidad de solventar problemas durante el procesamiento de datos, cuando ya no es posible mejorar o cambiar el criterio de muestreo.